Quantitative nonlinearity analysis of model-scale jet noise

Kyle G. Miller, Brent O. Reichman, Kent L. Gee, Tracianne B. Neilsen, and Anthony A. Atchley

Citation: AIP Conference Proceedings **1685**, 090003 (2015); doi: 10.1063/1.4934469
View online: http://dx.doi.org/10.1063/1.4934469
View Table of Contents: http://scitation.aip.org/content/aip/proceeding/aipcp/1685?ver=pdfcov
Published by the AIP Publishing

Quantitative Nonlinearity Analysis of Model-Scale Jet Noise

Kyle G. Miller[1,a)], Brent O. Reichman[1,b)], Kent L. Gee[1,c)],
Tracianne B. Neilsen[1,d)] and Anthony A. Atchley[2,e)]

[1]*Department of Physics and Astronomy, Brigham Young University, Provo, UT 84602, USA*
[2]*Graduate Program in Acoustics, The Pennsylvania State University, University Park, PA 16802, USA*

[a)]kglenmiller@gmail.com
[b)]brent.reichman@gmail.com
[c)]kentgee@byu.edu
[d)]tbn@byu.edu
[e)]atchley@psu.edu

Abstract. The effects of nonlinearity on the power spectrum of jet noise can be directly compared with those of atmospheric absorption and geometric spreading through an ensemble-averaged, frequency-domain version of the generalized Burgers equation (GBE) [B. O. Reichman et al., J. Acoust. Soc. Am. 136, 2102 (2014)]. The rate of change in the sound pressure level due to the nonlinearity, in decibels per jet nozzle diameter, is calculated using a dimensionless form of the quadspectrum of the pressure and the squared-pressure waveforms. In this paper, this formulation is applied to atmospheric propagation of a spherically spreading, initial sinusoid and unheated model-scale supersonic (Mach 2.0) jet data. The rate of change in level due to nonlinearity is calculated and compared with estimated effects due to absorption and geometric spreading. Comparing these losses with the change predicted due to nonlinearity shows that absorption and nonlinearity are of similar magnitude in the geometric far field, where shocks are present, which causes the high-frequency spectral shape to remain unchanged.

INTRODUCTION

Characterizing nonlinearity in jet noise has traditionally involved comparison of the power spectral density (PSD) along propagation radials. This approach not only necessitates several microphones placed far apart relative to the jet diameter, but the comparison naturally incorporates other effects that influence PSD evolution. Such effects include atmospheric absorption and geometric spreading from a directional, extended source, and in an outdoor measurement also ground reflections and wind and temperature gradients. These factors make it difficult to isolate nonlinear effects on PSD evolution. Other nonlinearity analysis techniques have been previously explored [1-3], but this paper focuses on the use of a quadspectral nonlinearity indicator to determine the presence and importance of nonlinearity with a measurement at a single location.

Morfey and Howell [4] introduced the dimensionless nonlinearity indicator known as "Q/S," based on the ensemble-averaged, frequency-domain version of the generalized Burgers equation for spherical spreading, absorption, and nonlinearity and defined as

$$\frac{Q}{S} = \frac{Q_{pp^2}}{p_{\mathrm{rms}} S_{pp}} = \frac{\mathrm{Im}\left\{\lim_{T\to\infty} \frac{1}{T} E\left[\mathcal{F}^*\{p(t)\}\mathcal{F}\{p^2(t)\}\right]\right\}}{p_{\mathrm{rms}} S_{pp}}, \tag{1}$$

where Q_{pp^2} is the quadspectral density between the pressure and squared pressure waveforms, S_{pp} is the pressure autospectral density, p_{rms} is the root-mean-square pressure, and $\mathcal{F}$ denotes a Fourier transform. Although Morfey and Howell and others have used Q/S and related indicators to demonstrate the presence of nonlinear propagation effects, a quantitative expression involving Q/S has been recently found [5] for the change in sound pressure level spectrum, L_p, with distance, r, that may be written as

Recent Developments in Nonlinear Acoustics
AIP Conf. Proc. 1685, 090003-1–090003-4; doi: 10.1063/1.4934469

$$\frac{\partial L_p}{\partial r} = -10\log_{10}(e)\cdot\left(\frac{2m}{r} + 2\alpha + \frac{\omega\beta p_{\mathrm{rms}}}{\rho_0 c_0^3}\frac{Q}{S}\right) = \nu_S + \nu_\alpha + \nu_N\,. \tag{2}$$

In Eq. (2), $10\log_{10}(e) \approx 4.34$; $m = 0$, 0.5, or 1 for planar, cylindrical, or spherical waves, respectively; α is the linear absorption coefficient; β is the coefficient of nonlinearity; ρ_0 is the equilibrium density of air; c_0 is the speed of sound; and ν_S, ν_α, and ν_N represent the frequency-dependent spatial rate of changes in L_p due to spreading, absorption, and nonlinearity, respectively.

Other analyses of jet noise have used Q/S to show the presence of nonlinearity [3, 6, 7], but have not been extended to the quantitative expression in Eq. (2), which has only treated analytical plane-wave cases [5]. This paper first presents a quantitative analysis of an initial sinusoid numerically propagated with spherical spreading and atmospheric absorption using a numerical implementation of the GBE [8]. Analysis of noise from an anechoic, laboratory scale, ideally expanded, Mach-2.0 unheated jet is also presented. Both analyses show that ν_N is largest in the near-field region, then becomes comparable to absorption and spreading in the far field.

SINUSOID PROPAGATION ANALYSIS

To create a simulation similar to the model-scale jet experiment, a sinusoidal waveform was propagated numerically using the GBE. Unlike the jet noise case, which exhibits range and frequency-dependent geometric spreading, spherical spreading is assumed at all distances. The distance is scaled with respect to a jet nozzle diameter (D_j), equal to 3.5 cm. The atmospheric conditions were taken to be the same as in the experiment, with temperature at 22.9°C, atmospheric pressure at 96.8 kPa, and relative humidity at 53%. The fundamental frequency of the wave was 4 kHz with amplitude of 22 kPa at 1 D_j, so as to approximate the rms amplitude of the jet data at 10 D_j. For accuracy in the calculations, a sampling frequency of 88 MHz was used with 2^{16} total samples. Figure 1(a) compares the nonlinearly propagated wave with the linear approximation (spreading and atmospheric absorption). Relative to linear propagation, significant wave steepening has occurred along with a slight decrease in the peak-to-peak pressure. Figure 1(b) shows the evolution of the harmonics in the waveform. Note the delayed onset of higher harmonics, with each harmonic reaching its maximum amplitude at successively larger distances from the source.

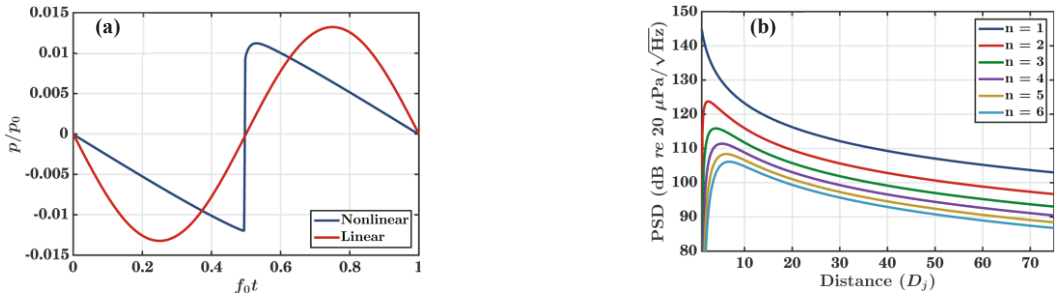

FIGURE 1. (a) Comparison of nonlinearly propagated wave at 75 D_j and the corresponding linear approximation. (b) Spectral amplitude of six harmonics. Each harmonic peaks at a successively larger distance from the source.

The calculations of ν_s, ν_α, and ν_N in Eq. (2) were carried out using the distance, frequency, assumed atmospheric conditions, and propagated waveform. The terms, along with their sum, are shown in Fig. 2 as a function of distance for the fundamental, second harmonic, and tenth harmonic. These two harmonics have frequencies similar to those analyzed in the jet noise case. In Fig. 2, a solid black line shows the sum of ν_s, ν_α, and ν_N, and the red circles represent the numerically calculated derivative from the curves in Fig. 1(b). The percent error between the two is less than 1% for all values shown. Very close to the source, ν_N is positive for all harmonics as they are first generated nonlinearly. However, nonlinear losses at the shock and energy transfer to even higher frequencies causes ν_N to eventually go negative for some of the harmonics, as seen in Fig. 2(b). For the tenth harmonic, ν_N decreases but remains positive away from the source. As pointed out by Blackstock [9], the harmonic amplitudes in a nonlinear wave undergoing unsteepening in the "old age" region decay more slowly than a linearly propagating wave. This difference is given by ν_N, which must remain nonzero out to very large distances.

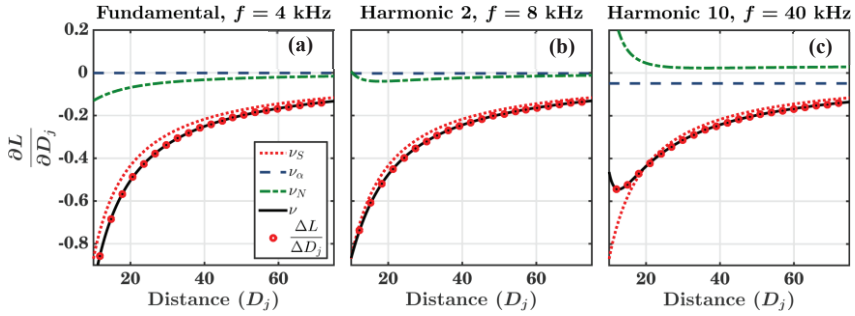

FIGURE 2. Comparison of $\boldsymbol{\nu}$ values for the fundamental, second harmonic, and tenth harmonic of the nonlinearly propagated waveform. Close to the source, harmonic strength is dominated by nonlinearity. Geometric spreading becomes the dominant effect at larger distances. For the tenth harmonic in (c), all three effects are of similar magnitude in the far field.

JET NOISE ANALYSIS

Laboratory-scale jet noise data were collected in an anechoic chamber on an ideally expanded, Mach-2.0, unheated jet of nozzle diameter 3.5 cm. Waveforms, sampled at 192 kHz, were acquired between 10-75 jet nozzle diameters (D_j) and 80° and 150° (relative to upstream axis) with a 3.18 mm and 6.35 mm microphone array whose origin was located 4 D_j downstream of the nozzle exit. This origin is upstream from the expected overall noise source region [10], but facility configuration constraints required this positioning. Figure 3(a) shows the measured power spectral densities (PSD) along 145°, which is the maximum far-field radiation angle. A shift in peak frequency is observed along the radial from 10 to 60 D_j, due to those microphones being in the geometric near field of a source with frequency-dependent source location, directivity, and spreading rate. It is important to note that this downward shift in peak frequency is not related to nonlinear effects (see discussion regarding Fig. 4 of Ref. [11]). For example, low-frequency noise is generated farther downstream from the nozzle than is high-frequency noise [10], so their propagation radials are different from each other and from the microphone array before converging at

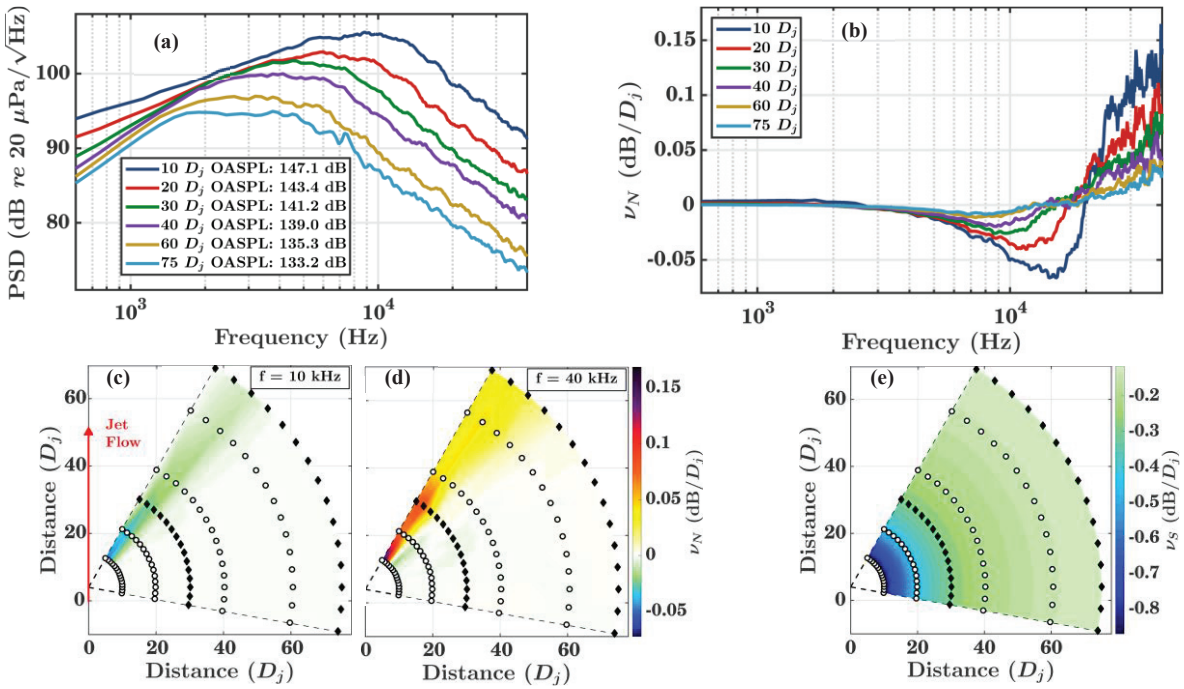

FIGURE 3. (a) Measured spectra along 145°, showing the downward frequency shift along the maximum far-field radiation angle. (b) Spectral plots for $\boldsymbol{\nu_N}$. A corresponding frequency shift occurs for where $\boldsymbol{\nu_N}$ changes sign. (c-d) Spatial maps of $\boldsymbol{\nu_N}$ for two different frequencies. Circles represent 3.18 mm mics and filled diamonds 6.35 mm mics. (e) Spatial map of $\boldsymbol{\nu_S}$ (constant with frequency), which is stronger than both nonlinearity and absorption.

~60 D_j. Between 10-20 kHz the roll-off changes from ~28 dB/octave at 10 D_j, the decay rate for large-scale structure radiation [12], to ~20 dB/octave, typical of shock-containing noise [13]. This spectral shape of the high frequencies remains fairly constant with distance, indicating that the energy losses due to absorption and energy gains due to nonlinearity are of similar magnitude; this is shown quantitatively below.

Figure 3(b) shows ν_N along the same radial. Negative and positive values of ν_N indicate loss of energy and gain in energy due to nonlinearity, respectively. The frequency at which the sign of ν_N changes from negative to positive tracks the downward trend in PSD peak frequency with propagation into the far field. The results indicate that the region of the spectrum with greatest amplitude at a given location drives nonlinear energy transfer to higher frequencies, similar to the sinusoid example shown previously. The spatial maps of ν_N in Figs. 3(c-d), created using a linear interpolation of the color scheme, quantitatively confirm that nonlinear effects are localized at angles near the maximum radiation direction, as indicated by prior analyses [6, 11, 14]. Along the principal radiation lobe, the energy loss rate (~ -0.01 to -0.05 dB/D_j) at 10 kHz and gain rate at 40 kHz (~ +0.03 to +0.1 dB/D_j) are very similar in magnitude to the sinusoid example. Similar to the numerically propagated sine wave, nonlinearity is more dominant than absorption close to the source, but the two effects are close to the same strength in the far field. Absorption gives a change of only -0.004 dB/D_j at 10 kHz and -0.05 dB/D_j at 40 kHz. Figure 3(d) shows a small negative region around the propagation radial at 130°, where energy is still being lost at 40 kHz. The peak frequency in this region is about twice that of the principle radiation radial, and energy is being lost at this frequency to higher harmonic generation. Figure 3(e) shows that ν_S, the change due to spherical spreading ($m = 1$), is stronger than both nonlinearity and absorption at all microphones in the tested region.

CONCLUSION

The Morfey-Howell [4] nonlinearity indicator, Q/S, has been extended to quantitative comparison of nonlinear effects with those of spreading and absorption for a spherically spreading, initially sinusoidal case and for supersonic model-scale jet noise. The analysis shows that nonlinearity is strongest close to the source, but approaches similar magnitude as absorption in the far field. Prior studies of the jet data have revealed that acoustic shocks form with propagation into the far field [14], and that the high-frequency spectral energy is increasingly due to the shocks [11]. This study confirms that the unchanging high-frequency spectral roll-off is due to comparable magnitudes of the loss due to absorption and the gain due to nonlinear generation as the shocks propagate.

ACKNOWLEDGMENTS

This work was supported by the U.S. Office of Naval Research.

REFERENCES

1. W. J. Baars, *et al.*, J. Fluid. Mech. **749**, 331-366 (2014).
2. S. A. McInerny, *et al.*, AIP Conf. Proc. **838**, 560-563 (2006).
3. S. A. McInerny and S. M. Ölçmen, J. Acoust. Soc. Am. **117**, 578-591 (2005).
4. C. L. Morfey and G. P. Howell, AIAA J. **19**, 986-992 (1981).
5. B. O. Reichman, *et al.*, "Quantitative analysis of a frequency-domain nonlinearity indicator," J. Acoust. Soc. Am. (submitted 2015).
6. K. L. Gee, *et al.*, AIP Conf. Proc. **1474**, 307-310 (2012).
7. B. P. Petitjean, *et al.*, International Journal of Aeroacoustics **5**, 193-215 (2006).
8. K. L. Gee, "Prediction of nonlinear jet noise propagation," Ph. D. Thesis, Pennsylvania State University, 2005.
9. D. T. Blackstock, AIP Conf. Proc. **838**, 601-606 (2006).
10. C. K. W. Tam, *et al.*, J. Fluid. Mech. **615**, 253-292 (2008).
11. K. L. Gee, *et al.*, J. Acoust. Soc. Am. **128**, EL211-EL216 (2010).
12. T. B. Neilsen, *et al.*, J. Acoust. Soc. Am. **133**, 2116-2125 (2013).
13. S. N. Gurbatov and O. V. Rudenko, "Statistical phenomena," in *Nonlinear Acoustics*, (American Press, San Diego, 1998), pp. 377-398.
14. K. L. Gee, *et al.*, J. Acoust. Soc. Am. **133**, EL491-EL497 (2013).